Multiple scattering effects in Glauber model descriptions of single-nucleon removal reactions

Rui-Ying Chen,[1] Dan-Yang Pang,[1,2,*] Cen-Xi Yuan,[3] Yi-Ping Xu,[4]
Wen-Di Chen,[1] Wen-Long Hai,[1] Jing-Jing Yan,[1] and Wei-Jia Kong[1]

[1]*School of Physics, Beihang University, Beijing 100191, China*
[2]*Beijing Key Laboratory of Advanced Nuclear Materials and Physics, Beihang University, Beijing 100191, China*
[3]*Sino-French Institute of Nuclear Engineering and Technology, Sun Yat-Sen University, Zhuhai 519082, China*
[4]*School of Nuclear Science and Engineering, North China Electric Power University, Beijing 102206, China*

The Glauber/eikonal model is a widely used tool for study of intermediate- and high-energy nuclear reactions. When calculating the Glauber/eikonal model phase-shift functions, the optical limit approximation (OLA) is often used. The OLA neglects the multiple scattering of the constituent nucleons in the projectile and the target nuclei. On the other hand, the nucleon-target version of the Glauber model (the NTG model) proposed by B. Abu-Ibrahim and Y. Suzuki includes multiple scattering effects between the projectile nucleons and the target nuclei. The NTG model has been found to improve the description of the elastic scattering angular distributions and the total reaction cross sections of some light heavy-ion systems with respect to the OLA. In this work, we study the single-nucleon removal reactions (SNRR) induced by carbon isotopes on ^{12}C and ^{9}Be targets using both the NTG model and the OLA. Reduction factors (RFs) of the single nucleon spectroscopic factors are obtained by comparing the experimental and theoretical SNRR cross sections. It is found that, on average, the RFs obtained with the NTG model is smaller than those using the OLA by 7.8%, in which, the averaged differences in one-neutron removal is 10.6% and those in one-proton removal is 4.2%. But the RFs still have a strong dependence on the neutron-proton asymmetry ΔS of the projectile nuclei even when the NTG model is used.

Keywords: Glauber model of nuclear reactions, single-nucleon removal reactions, spectroscopic factors

I. INTRODUCTION

Measurements and theoretical analysis of single-nucleon removal reactions are of great value for studies of single-particle strengths of atomic nuclei, which are quantitatively represented by spectroscopic factors (SFs) [1]. It is well-known that the SFs extracted from $(e, e'p)$ and single-nucleon transfer reactions are found to be $30\% - 50\%$ smaller than those predicted by configuration interaction shell model (CISM) [2, 3]. Such reduction or quenching of SFs, represented by the quenching factors, R_s, is supposed to be originated from the limited model spaces and insufficient treatment of the nucleon-nucleon correlations in the traditional CISM [4, 5]. Unlike the results from $(e, e'p)$ reactions, from single-nucleon transfer reactions, and from $(p, 2p)$ and (p, pn) reactions [2, 3, 6, 7], where the R_s values of different nuclei are nearly constant, the quenching factors from intermediate energy single-nucleon removal reactions are found to depend almost linearly with the proton-neutron asymmetry of the atomic nuclei, ΔS ($\Delta S = S_p - S_n$ for proton removal and $\Delta S = S_n - S_p$ for neutron removal with S_n and S_p being the neutron and proton separation energies in the ground states of the projectile nuclei, respectively) [8, 9]. For cases when ΔS is larger than around 20 MeV, which correspond to removal of strongly bound nucleons, the R_s values decrease to about 0.3; however, when ΔS is smaller than around -20 MeV, which corresponds to removal of weakly-bound nucleons, the R_s values are close to unity. The reasons why such a clear linear dependence is seen in results of intermediate-energy single-nucleon removal reactions are still not known. Since most of the single-nucleon removal reactions are analyzed with the Glauber model, validity of the eikonal/Glauber model [8–10] has been put under question [11].

Because of its simplicity, the optical limit approximation (OLA) is often used in the eikonal/Glauber model analysis of the intermediate- and high-energy nuclear reactions [10, 12, 13]. Only the first-order term of the expansion of the full Glauber phase shift is taken into account with the OLA. Higher-order interactions, such as the nucleon-nucleon multiple scattering processes are neglected [14]. In Ref. [15], B. Abu-Ibrahim and Y. Suzuki found that although the Glauber model with the OLA can reasonably reproduce the total reaction cross sections of some stable ions on ^{9}Be, ^{12}C, ^{27}Al targets, it failed to reproduce the reaction cross sections and elastic scattering angular distributions of unstable nuclei. For this, they proposed to calculate the projectile-target phase shifts using nucleon-target interactions in Glauber model calculations. This so-called NTG model (nucleon-target version of the Glauber model) has been found to improve the description of the reaction cross sections and the elastic scattering angular distributions data considerably [15–17]. However, to our knowledge, application of the NTG model to the analysis of single-nucleon knockout reactions and to study its influence on the reduction factors of single particle strengths has not been made yet. In this work, we study how much the R_s values of single-nucleon knockout reactions change when the NTG model is used instead of the usual OLA. Since the NTG model includes multiple scattering effects in the phase-shift functions of the colliding systems with respect to the OLA, we expect this work may give us information about how much the multiple scattering effects will affect the description of single nucleon removal reactions using the Glauber model.

This paper is organized as the following: the NTG model and the OLA of the Glauber model are briefly introduced in

* Corresponding author: dypang@buaa.edu.cn

section II; results of our calculations are given in section III, which include 1) examination of the NTG model about its reproduction of the elastic scattering and total reaction cross section data. The cases studied are the angular distributions of ^{12}C elastic scattering from a carbon target at incident energies from 30 to 200 MeV/u and the ^{12}C+^{12}C total reaction cross sections from 20 to 1000 MeV/nucleon, 2) detailed study of the NTG model on single-nucleon removal at different incident energies, the case studied here is the ^{9}Be(^{19}C,^{18}C)X reaction, and 3) effects of the NTG model on the reduction factors of the single particle strengths. The cases studied are single nucleon removal cross sections of carbon isotopes $^{9,10,12-20}$C on ^{9}Be and carbon targets within 43-250 MeV/nucleon incident energies. The range of ΔS covered in these reactions is from -26.6 to 20.1 MeV. All results are compared with those of the OLA calculations in order to explicate the influence of multiple scattering effects in these reactions. The conclusions are given in section IV.

II. THE NTG MODEL AND THE OLA

The NTG model was introduced in Refs. [15, 16]. Details of its formulae can be found in Ref. [14]. For the convenience of the readers, we recapitulate the necessary ones here. Let us start from the phase-shift function of a nucleon-target system, χ_{NT}, which is defined in the Glauber model framework as [14]:

$$e^{i\chi_{NT}(\boldsymbol{b})} = \langle \Phi_0^{\mathrm{T}} | \prod_{j=1}^{A_{\mathrm{T}}} [1 - \Gamma_{NN}(\boldsymbol{b} - \boldsymbol{t}_j)]\, \Phi_0^{\mathrm{T}} \rangle, \quad (1)$$

where $\boldsymbol{b}$ is the impact factor vector, $\boldsymbol{t}_j$ is the projection vector of the position of the jth nucleon in the target nucleus on the x-y plane (the beam direction being the z-axis), Γ_{NN} is the nucleon-nucleon (NN) profile function, which is the Fourier transform of the NN scattering amplitude, and $|\Phi_0\rangle$ is the wave function of the target nucleus, which has a mass number A_{T}. When an independent particle model wave function is used, which is usually assumed in Glauber model calculations, the density of the target nucleus can be written as[14]:

$$|\Phi_0^{\mathrm{T}}(\boldsymbol{r}_1, \boldsymbol{r}_2, \cdots, \boldsymbol{r}_{A_{\mathrm{T}}})|^2 = \prod_{j=1}^{A_{\mathrm{T}}} n_j(\boldsymbol{r}_j), \quad (2)$$

where $n_j(\boldsymbol{r}_j)$ stands for the normalized density distribution of the jth nucleon in the target nucleus. The nucleon density distribution is then

$$\rho_{\mathrm{T}}(\boldsymbol{r}) = \sum_{j=1}^{A_{\mathrm{T}}} n_j(\boldsymbol{r}). \quad (3)$$

With an uncorrelated wave function satisfying Eq. 2, the nucleon-target phase shift function has the form [14]:

$$e^{i\chi_{NT}(\boldsymbol{b})} = \prod_{j=1}^{A_{\mathrm{T}}} \left[1 - \int d\boldsymbol{r} n_j(\boldsymbol{r}) \Gamma_{NN}(\boldsymbol{b} - \boldsymbol{t})\right], \quad (4)$$

where $\boldsymbol{t}$ is the projection of $\boldsymbol{r}$ on the x-y plane. When the range of the NN interaction is smaller than the radius of the target nucleus, which is satisfied in most cases, the integral $\int d\boldsymbol{r} n_j(\boldsymbol{r}) \Gamma_{NN}(\boldsymbol{b} - \boldsymbol{t})$ will be smaller than unity [14]. Then the following approximation could be made [14]:

$$1 - \int d\boldsymbol{r} n_j(\boldsymbol{r}) \Gamma_{NN}(\boldsymbol{b} - \boldsymbol{t}) \approx e^{-\int d\boldsymbol{r} n_j(\boldsymbol{r}) \Gamma_{NN}(\boldsymbol{b} - \boldsymbol{t})}. \quad (5)$$

One then gets the nucleon-target phase shift of the OLA [14]:

$$\begin{aligned} e^{i\chi_{NT}^{\mathrm{OLA}}(\boldsymbol{b})} &= \prod_{j=1}^{A_{\mathrm{T}}} \exp\left[-\int d\boldsymbol{r} n_j(\boldsymbol{r}) \Gamma_{NN}(\boldsymbol{b} - \boldsymbol{t})\right] \\ &= \exp\left[-\sum_{j=1}^{A_{\mathrm{T}}} \int d\boldsymbol{r} n_j(\boldsymbol{r}) \Gamma_{NN}(\boldsymbol{b} - \boldsymbol{t})\right] \\ &= \exp\left[-\int d\boldsymbol{r} \rho_T(\boldsymbol{r}) \Gamma_{NN}(\boldsymbol{b} - \boldsymbol{t})\right]. \end{aligned} \quad (6)$$

This results in the nucleon-nucleus phase-shift function using the OLA being:

$$\chi_{NT}^{\mathrm{OLA}}(\boldsymbol{b}) = i \int d\boldsymbol{r} \rho_T(\boldsymbol{r}) \Gamma_{NN}(\boldsymbol{b} - \boldsymbol{t}). \quad (7)$$

Note that in Eqs. (1) and (4), multiple scattering terms appear through cumulant expansions of the phase-shift functions. However, after applying the approximation of Eq. (5) in Eq. (4), the resulting nucleon-nucleus phase-shift with the OLA in Eq. (7) contains no multiple scattering terms anymore [18].

Similar to the nucleon-nucleus case in Eq. (1), the nucleus-nucleus phase shift function, $\chi_{PT}(\boldsymbol{b})$, for a composite projectile and a target nucleus is [14]:

$$e^{i\chi_{PT}(\boldsymbol{b})} = \langle \Phi_0^{\mathrm{P}} \Phi_0^{\mathrm{T}} | \prod_{i=1}^{A_{\mathrm{P}}} \prod_{j=1}^{A_{\mathrm{T}}} [1 - \Gamma_{NN}(\boldsymbol{b} + \boldsymbol{s}_i - \boldsymbol{t}_j)] | \Phi_0^{\mathrm{P}} \Phi_0^{\mathrm{T}} \rangle, \quad (8)$$

where Φ_0^{P} is the many-body wave functions of the projectile (with a mass number A_{P}) in its ground state. The integrals are over the coordinates of all the nucleons i and j in the projectile and target nuclei, whose coordinates are $\boldsymbol{r}_i$ and $\boldsymbol{r}_j$, respectively. $\boldsymbol{s}_i$, and $\boldsymbol{t}_j$ are their projections on the x-y plane. The nucleus-nucleus phase shift in this equation contains contributions from single collisions and all order multiple scattering among the constituent nucleons in the projectile and the target nuclei. Equation (8) is cumbersome to evaluate directly even if it is possible. So the optical limit approximation is usually used and the phase shift function with this approximation is [14]:

$$\chi_{\mathrm{PT}}^{\mathrm{OLA}}(\boldsymbol{b}) = i \int d\boldsymbol{r}_{\mathrm{P}} \rho_{\mathrm{P}}(\boldsymbol{r}_{\mathrm{P}}) \int d\boldsymbol{r}_{\mathrm{T}} \rho_{\mathrm{T}}(\boldsymbol{r}_{\mathrm{T}}) \Gamma_{NN}(\boldsymbol{b} + \boldsymbol{s} - \boldsymbol{t}), \quad (9)$$

where ρ_{P} and ρ_{T} are the nucleon density distributions of the projectile and the target nuclei, respectively, $\boldsymbol{r}_{\mathrm{P}}$ and $\boldsymbol{r}_{\mathrm{T}}$ are the positions of their constituent nucleons, whose projections

on the x-y plane are $\boldsymbol{s}$ and $\boldsymbol{t}$ respectively. As in the nucleon-nucleus case in Eq. (7), only single NN collisions contribute to this phase shift. Contributions from multiple scatterings are missing, which could be, to some extent, recovered by the nucleon-target version of the Glauber model (the NTG model) proposed by Abu-Ibrahim and Suzuki [14–17].

The idea of the NTG model is to replace $\langle\Phi_0^{\mathrm{T}}|\prod_{j\in\mathrm{T}}[1-\Gamma_{NN}(\boldsymbol{b}+\boldsymbol{s}_i-\boldsymbol{t}_j)]|\Phi_0^{\mathrm{T}}\rangle$ for each nucleon i in the projectile in Eq. (8) by

$$\begin{aligned}
&\langle\Phi_0^{\mathrm{T}}|\prod_{j=1}^{A_{\mathrm{T}}}[1-\Gamma_{NN}(\boldsymbol{b}+\boldsymbol{s}_i-\boldsymbol{t}_j)]|\Phi_0^{\mathrm{T}}\rangle \\
&\equiv 1-\Gamma_{NT}\left(\boldsymbol{b}+\boldsymbol{s}_i\right), \qquad (10)
\end{aligned}$$

where $\Gamma_{NT}\left(\boldsymbol{b}+\boldsymbol{s}_i\right)$ is the profile function of its collision with the target nucleus. The nucleus-nucleus phase shift then takes the form [14]:

$$e^{i\chi_{PT}^{\mathrm{NTG}}(\boldsymbol{b})}=\langle\Phi_0^{\mathrm{P}}|\prod_{i=1}^{A_{\mathrm{P}}}\left[1-\Gamma_{NT}\left(\boldsymbol{b}+\boldsymbol{s}_i\right)\right]|\Phi_0^{\mathrm{P}}\rangle. \qquad (11)$$

This is the so-called NTG model. Following the same procedure of obtaining the Eq. (7), the phase shift of the projectile-target system with the NTG model is:

$$\chi_{PT}^{\mathrm{NTG}}(\boldsymbol{b})=i\int d\boldsymbol{r}\rho_{\mathrm{P}}(\boldsymbol{r})\Gamma_{NT}(\boldsymbol{b}+\boldsymbol{s}), \qquad (12)$$

and the nucleon-target profile function, Γ_{NT} is:

$$\begin{aligned}
&\Gamma_{NT}(\boldsymbol{b}+\boldsymbol{s}_i) \\
&=1-\langle\Phi_0^{\mathrm{T}}|\prod_{j=1}^{A_{\mathrm{T}}}[1-\Gamma_{NN}(\boldsymbol{b}+\boldsymbol{s}_i-\boldsymbol{t}_j)]|\Phi_0^{\mathrm{T}}\rangle \\
&=1-\exp\left[-\int d\boldsymbol{r}_T\rho_T(\boldsymbol{r}_T)\Gamma_{NN}(\boldsymbol{b}+\boldsymbol{s}-\boldsymbol{t})\right]. \qquad (13)
\end{aligned}$$

Substituting this Γ_{NT} in Eq. (12), we get the nucleus-nucleus phase shift function of the NTG model:

$$\begin{aligned}
&\chi_{PT}^{\mathrm{NTG}}(\boldsymbol{b})=i\int d\boldsymbol{r}_{\mathrm{P}}\rho_{\mathrm{P}}(\boldsymbol{r}_{\mathrm{P}}) \\
&\times\left\{1-\exp\left[-\int d\boldsymbol{r}_{\mathrm{T}}\rho_{\mathrm{T}}(\boldsymbol{r}_{\mathrm{T}})\Gamma_{NN}(\boldsymbol{b}+\boldsymbol{s}-\boldsymbol{t})\right]\right\} \qquad (14)
\end{aligned}$$

That the nucleus-nucleus phase shift of the NTG model contains multiple scattering effects other than the OLA can be seen by power expansion of the nucleon-target profile function of Eq. (13):

$$\begin{aligned}
&\Gamma_{NT}(\boldsymbol{b}+\boldsymbol{s}_i) \\
&=\int d\boldsymbol{r}_T\rho_T(\boldsymbol{r}_T)\Gamma_{NN}(\boldsymbol{b}+\boldsymbol{s}-\boldsymbol{t})- \\
&\frac{1}{2!}\left[\int d\boldsymbol{r}_T\rho_T(\boldsymbol{r}_T)\Gamma_{NN}\left(\boldsymbol{b}+\boldsymbol{s}-\boldsymbol{t}\right)\right]^2+\cdots. \qquad (15)
\end{aligned}$$

The first term is contributed by single scattering of the projectile nucleon from nucleons in the target nucleus. The second and other terms represent contributions from multiple NN scattering [14]. Clearly, if only the first term is used in Eq. (12), the NTG phases shift will reduce to that of the OLA in Eq. (9). By taking into account the higher order terms in Eq. (15), phase shifts with the NTG model recover some multiple scattering effects that are missing with the OLA. One should note, however, that the contributions from multiple scattering processes included in this way is not identical to those in full Glauber model in Eqs. (1) and (8) [19]. Nevertheless, as we will show in the next section, the NTG model could improve the description of the elastic scattering angular distributions, especially at low incident energies, and total reaction cross sections for the ^{12}C+^{12}C test case within a rather wide range of incident energies. Practically, a symmetrized version of the NTG phase shift is often calculated [15, 17]:

$$\begin{aligned}
\chi_{PT}^{\mathrm{NTG}}(\boldsymbol{b}) &= \frac{i}{2}\int d\boldsymbol{r}_{\mathrm{P}}\rho_{\mathrm{P}}(\boldsymbol{r}_{\mathrm{P}})\Big\{1- \\
&\exp\left[-\int d\boldsymbol{r}_{\mathrm{T}}\rho_{\mathrm{T}}(\boldsymbol{r}_{\mathrm{T}})\Gamma_{NN}(\boldsymbol{b}+\boldsymbol{s}-\boldsymbol{t})\right]\Big\} \\
&+\frac{i}{2}\int d\boldsymbol{r}_{\mathrm{T}}\rho_{\mathrm{T}}(\boldsymbol{r}_{\mathrm{T}})\Big\{1- \\
&\exp\left[-\int d\boldsymbol{r}_{\mathrm{P}}\rho_{\mathrm{P}}(\boldsymbol{r}_{\mathrm{P}})\Gamma_{NN}(\boldsymbol{b}+\boldsymbol{t}-\boldsymbol{s})\right]\Big\}.
\end{aligned} \qquad (16)$$

However, the phase-shifts calculated with Eqs. (14) and (16) are often very close to each other [15, 16].

The profile function Γ_{NN} in the both the OLA and the NTG model calculations is parameterized in a Gaussian form:

$$\Gamma_{pN}\left(\mathbf{b}\right)=\frac{1-i\alpha_{pN}}{4\pi\beta_{pN}}\sigma_{pN}^{\mathrm{tot}}\exp\left(-\frac{\mathbf{b}^2}{2\beta_{pN}}\right), \qquad (17)$$

where the Γ_{NN} parameters $\sigma_{pN}^{\mathrm{tot}}$, α_{pN}, and β_{pN} are the proton-nucleon total cross section, the ratio of the real to imaginary part of the p-N scattering amplitudes, and the corresponding slope parameter [20], respectively. Due to the lack of experimental data on neutron-neutron scattering, Γ_{pp} is commonly used instead of Γ_{NN}. In this work, $\sigma_{pN}^{\mathrm{tot}}$ are taken from Ref. [21], which is parameterized by fitting the experimental data from Ref. [22], the α_{pN} parameters are taken from those tabulated from Ref. [20] for a range of incident energies from 100 to 2200 MeV/u. If the beam energy is lower than 100 MeV/u, we take the value corresponding to lowest energy from the table. The finite range slope parameters β_{pN} are taken to be 0.125 fm^2, in accordance with systematic studies of single-nucleon removal reaction[10, 12, 23].

III. COMPARISONS BETWEEN THE NTG MODEL AND OLA IN GLAUBER MODEL CALCULATIONS

In Ref. [24], T. Nagashisa and W. Horiuchi demonstrated the effectiveness of the NTG by comparing the description of the total reaction cross sections using the full Glauber model calculation, the NTG model, and the OLA for cases of ^{12,20,22}C on a ^{12}C target at various incident energies. In this work, our main purpose is to study how much the single-nucleon removal cross sections (σ_{-1N}) will change when the

NTG model instead of the OLA is used. Before calculating σ_{-1N}, we need to firstly compare our calculations for the elastic scattering angular distributions and total reaction cross sections with experimental data and with the predictions of the OLA. The calculations are made for the ^{12}C+^{12}C system. By doing so, we also verify the effectiveness of the Γ_{NN} parameters used in our calculations, which are further used in the calculations of σ_{-1N}. The single-nucleon removal reactions are calculated using a modified version of the computer code MOMDIS [25].

A. Elastic scattering angular distributions and total reaction cross sections

The angular distributions of ^{12}C elastic scattering from a ^{12}C target at 30, 85, 120, and 200 MeV/nucleon are calculated with both the OLA and the NTG model. The results are shown in Fig. 1 together with the experimental data. Clearly, the NTG improved the description of the ^{12}C+^{12}C elastic scattering considerably with respect to the OLA, especially when the incident energy is below around 100 MeV/nucleon. This can be expected because the multiple scattering effect, which are included in the NTG model but not in the OLA, should be more important at low incident energies than at higher incident energies. Note that other corrections due to, for instance, the antisymmetrization of the projectile and target wavefunctions [26], the Fermi motion of the nucleons in the colliding nuclei [27], distortion of the trajectories [28], can also affect the low-energy cross sections. More complete calculations taking these aspect together might be an interesting subject for future.

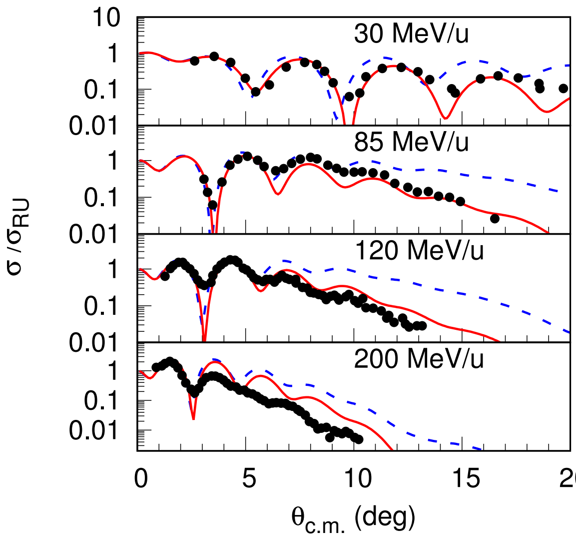

Fig. 1. Elastic scattering angular distributions of ^{12}C on a carbon target at incident energies of 30, 85, 120, and 200 MeV/nucleon. The red solid and blue dashed curves are results of Glauber model calculations with the NTG model and the OLA, respectively. The dots are experimental data from Refs. [29, 30].

Comparison between the NTG and OLA predictions to the total reaction cross sections of the ^{12}C+^{12}C system is shown in Fig. 2. Again, we see that results of the NTG model have better agreement with the experiment data than those of the OLA, especially for the incident energies at several tens of MeV/nucleon and above, where most of the one-nucleon removal cross section data were measured [9]. In both elastic scattering and total reaction cross section calculations, the proton and neutron density distributions of the ^{12}C nucleus are taken to be a Gaussian form with a root-mean-square radius of 2.32 fm [9], which is very close to the 2.33 ± 0.01 fm from elastic electron scattering data [31].

Note that the Γ_{NN} parameters are the same in both NTG and OLA calculations. The only difference between these two methods is that the former introduced multiple scattering effects in the calculation of eikonal phase functions. The improvement provided by the NTG model in the description of elastic scattering angular distributions and the total reaction cross sections suggests that nuclear medium effects, such as the multiple scattering effect studied here, should be taken into account in Glauber model description of the nuclear reactions induced by heavy-ions. In the following section, we study how the NTG model could affect the theoretical predictions of the single-neutron removal cross sections and the single particle strengths obtained from the experimental data.

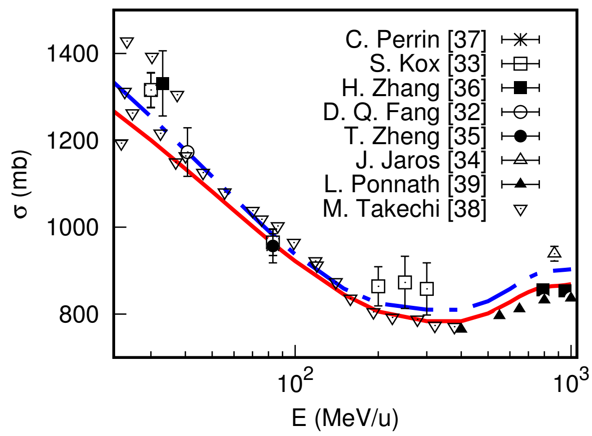

Fig. 2. Reaction cross sections of ^{12}C on a carbon target. The red solid and blue dash-dotted curves are results of Glauber model calculations with the NTG model and the OLA, respectively. The symbols represent experimental data from Ref. [32–39].

B. Single-nucleon removal cross sections at different incident energies

In an inclusive single-nucleon removal reaction, $\mathrm{A(a, b)X}$, where only the core nucleus b ($\mathrm{A_b} = \mathrm{A_a} - 1$) is detected, two processes may happen: the diffraction dissociation and stripping, which correspond to the valence neutron escaped or being captured by the target nucleus, respectively. Within the Glauber model framework, their cross sections, $\sigma_{sp}^{\rm dd}$ and $\sigma_{sp}^{\rm str}$,

respectively, are calculated by: [40]:

$$\sigma_{sp}^{\rm dd} = \frac{1}{2j+1}\sum_{m}\int d\mathbf{b}\left[\left\langle\psi_{nljm}\left||1-S_vS_c|^2\right|\psi_{nljm}\right\rangle - \sum_{m'}\left|\langle\psi_{nljm'}\left|(1-S_vS_c)\right|\psi_{nljm}\rangle\right|^2\right], \tag{18}$$

and

$$\sigma_{sp}^{\rm str} = \frac{1}{2j+1}\sum_{m}\int d\mathbf{b}\,|S_c|^2 \times \left\langle\psi_{nljm}\left|\left(1-|S_v|^2\right)\right|\psi_{nljm}\right\rangle. \tag{19}$$

Here $S_c = e^{i\chi_{cT}}$ and $S_v = e^{i\chi_{vT}}$ are the core-target and the valence nucleon-target S-matrices, respectively. The valence nucleon-target phase shift function χ_{vT} is calculated with Eq. (7), and the core-target phase shift function χ_{cT} is calculated according to Eq. (9) for the OLA and Eq. (16) for the NTG model; $\boldsymbol{b}$ is the impact factor vector of the projectile in the plane perpendicular to the beam direction, ψ_{nljm} is the single-particle wave function (SPWF) with n, l, and j being the principal, the angular momentum, and the total angular momentum numbers respectively, and m is the projection of j. Equations (7, 9, 14 and 16) are about nuclear phase-shift only. For charged particles, one also has to include the Coulomb phase-shift [25]:

$$\chi_{\rm C} = 2\eta\ln(kb), \tag{20}$$

where $\eta = Z_1Z_2e^2\mu/\hbar^2k$ is the Sommerfeld parameter with Z_1 and Z_2 being the charge numbers of the two colliding particles, whose reduced mass is μ, and k being the wave number in the center of mass system. The single-particle wave functions are associated with the specific states of the core with spin I_b and the composite nuclei with spin I_a by spectroscopic factors, $(C^2S)_{I_aI_b,nlj}$. So, the single-particle cross section of removal of a nucleon from the ground state of a projectile leaving the core nucleus in a specific state with the SPWF having quantum numbers nlj is:

$$\sigma_{sp}(I_aI_b,nlj) = \left(\frac{\rm A}{\rm A-1}\right)^N (C^2S)_{I_aI_b,nlj}\times(\sigma_{sp}^{dd}+\sigma_{sp}^{str}), \tag{21}$$

where the $[A/(A-1)]^N$ factor is for the center-of-mass corrections to the spectroscopic factor C^2S [41], and $N = 2n+l$ is the number of oscillator quanta associated with the major shell of the removed particle (the minimum value of n is taken to be zero).

Experimentally, single-nucleon removal cross sections are usually measured inclusively, namely, only the core nucleus b is measured without discriminating its energy states. Correspondingly, theoretical calculations for these measurements should also include the contributions from all the bound excited states of the core nucleus b [10], which corresponds to summation of all the single-particle cross sections associated with all possible single particle wave functions:

$$\sigma_{-1N}^{\rm th} = \sum_{nlj,I_b}\sigma_{sp}(I_aI_b,nlj). \tag{22}$$

TABLE 1. Single neutron removal cross sections of ^{19}C on a beryllium target at incident energies of 64, 100, 200, and 400 MeV/nucleon calculated with the NTG model, $\sigma_{-1n}^{\rm NTG}$, and the OLA, $\sigma_{-1n}^{\rm OLA}$. The state of the core nucleus and their corresponding single-nucleon spectroscopic factors are taken from Ref. [12].

$E_{\rm inc}$	E_x	J^π	nlj	C^2S	$\sigma_{-1n}^{\rm OLA}$	$\sigma_{-1n}^{\rm NTG}$	$\sigma_{-1n}^{\rm NTG}/\sigma_{-1n}^{\rm OLA}$
64	0.000	0^+	$1s_{1/2}$	0.580	104.31	109.3	1.050
	2.144	2^+	$0d_{5/2}$	0.470	18.93	21.16	1.118
	3.639	2^+	$0d_{5/2}$	0.104	3.53	3.98	1.127
	3.988	0^+	$1s_{1/2}$	0.319	17.82	19.72	1.107
	4.915	3^+	$0d_{5/2}$	1.523	46.18	52.21	1.131
	4.975	2^+	$0d_{5/2}$	0.922	27.83	31.46	1.130
	Inclusive				218.42	237.83	1.089
100	0.000	0^+	$1s_{1/2}$	0.580	87.58	90.14	1.029
	2.144	2^+	$0d_{5/2}$	0.470	17.95	19.13	1.066
	3.639	2^+	$0d_{5/2}$	0.104	3.41	3.64	1.067
	3.988	0^+	$1s_{1/2}$	0.319	16.43	17.44	1.061
	4.915	3^+	$0d_{5/2}$	1.523	45.05	48.24	1.071
	4.975	2^+	$0d_{5/2}$	0.922	27.15	29.08	1.071
	Inclusive				197.57	207.67	1.051
200	0.000	0^+	$1s_{1/2}$	0.580	61.66	63.55	1.031
	2.144	2^+	$0d_{5/2}$	0.470	15.46	16.52	1.069
	3.639	2^+	$0d_{5/2}$	0.104	3.01	3.23	1.073
	3.988	0^+	$1s_{1/2}$	0.319	13.47	14.30	1.062
	4.915	3^+	$0d_{5/2}$	1.523	40.59	43.61	1.071
	4.975	2^+	$0d_{5/2}$	0.922	24.48	26.31	1.075
	Inclusive				158.67	167.52	1.056
400	0.000	0^+	$1s_{1/2}$	0.580	54.76	57.04	1.042
	2.144	2^+	$0d_{5/2}$	0.470	14.61	16.00	1.095
	3.639	2^+	$0d_{5/2}$	0.104	2.87	3.16	1.101
	3.988	0^+	$1s_{1/2}$	0.319	12.54	13.57	1.082
	4.915	3^+	$0d_{5/2}$	1.523	38.80	42.91	1.106
	4.975	2^+	$0d_{5/2}$	0.922	23.41	25.89	1.106
	Inclusive				146.99	158.57	1.079

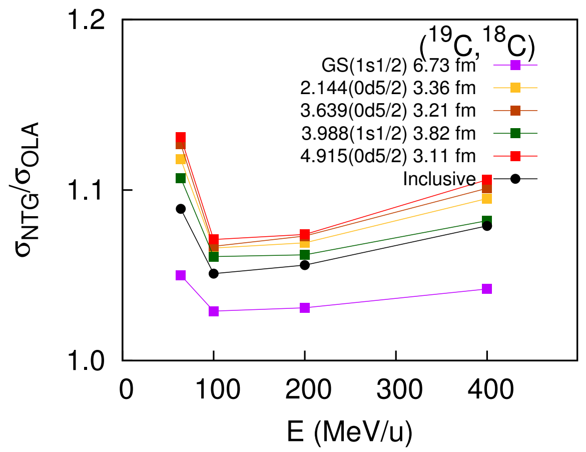

Fig. 3. Ratios of the NTG and OLA predicted single particle cross sections associated with different core states of the ^{9}Be(^{19}C,^{18}C)X reaction at incident energies 64, 100, 200, and 400 MeV/nucleon. The black dots represent the results calculated with Eq. (22). The excitation energies of the core nucleus ^{18}C and the properties of their corresponding single-particle wave functions – their nlj values and root-mean-square radii – are also shown. The lines are to guide eyes.

In order to see how much difference the NTG model predicts the single-nucleon removal cross sections with respect to the OLA, we study the (^{19}C,^{18}C) reaction on a ^{9}Be target at 64, 100, 200, and 400 MeV/nucleon incident energies. The excited states of the ^{18}C nucleus, the associated single particle wave functions, and their corresponding shell model predicted spectroscopic factors are taken to be the same as those in Ref. [12]. The single particle wave functions are calculated with single particle potentials of Woods-Saxon forms with the depths adjusted to provide the experimental separation energies of the valence nucleon, and the radius and diffuseness parameters are taken to be $r_0 = 1.25$ fm and $a = 0.7$ fm, respectively, the same as those used in Ref. [12]. The results are shown in Table. 1. Single-nucleon removal cross sections with the NTG model and the OLA are denoted as $\sigma_{-1n}^{\mathrm{NTG}}$ and $\sigma_{-1n}^{\mathrm{OLA}}$, respectively. Note that the $\sigma_{-1n}^{\mathrm{OLA}}$ values at 64 MeV/nucleon agree very well with those reported in Ref. [12]. The ratios between $\sigma_{-1n}^{\mathrm{NTG}}$ and $\sigma_{-1n}^{\mathrm{OLA}}$, are also depicted in Fig. 3.

It is interesting to observe that:

1. the one-nucleon removal cross sections calculated with the NTG model is larger than those with the OLA within the whole energy range from 50 to 400 MeV/nucleon,

2. Such differences are larger at incident energies smaller than around 100 MeV/nucleon, almost constant around 100-200 MeV/nucleon, and increase slightly when the incident energy is larger than around 200 MeV/nucleon,

3. The differences are also bigger when the root-mean-square radius of the single particle wave function is smaller, which means that the NTG model is especially important for one-neutron removal cross sections of a given reaction when the single nucleon is tightly bound.

The same are found for other nuclei studied in this work. The difference between the NTG model and the OLA is in the core-target S-matrix, S_c, only. However, as we see from Eqs. (18) and (19), we are not able to separate S_c from S_v and the single particle wave functions in the calculation of single-nucleon removal cross sections. Thus, we can not exhibit the details how the NTG model along affects the σ_{-1n} values with respect to the OLA. In the following subsection, we study how the spectroscopic factors extracted from the experimental data and their reduction factors change when the NTG model instead of the OLA is used.

C. Reduction factors of single particle strengths

The spectroscopic factors in Eq. (22) are often taken from configuration interaction shell model (CISM) calculations in calculating the one-nucleon removal cross sections. Due to limited model spaces and insufficient treatment of nucleon-nucleon correlations, It is well-known that the CISM predicted SFs are usually larger than the experimental ones. Reduction factors of the SFs, R_s, which are ratios between the experimental and theoretical SFs, are defined to quantify such differences. For the case of inclusive single-nucleon knockout reactions, the reduction factors are defined as the ratios between the experimental and theoretical cross sections [8, 9]:

$$R_s = \sigma_{-1N}^{\mathrm{exp}}/\sigma_{-1N}^{\mathrm{th}}.$$

For nuclei that have more than one sets of experimental data available, a weighted mean of the R_s values for each measurement is used [43]:

$$\mathfrak{R} = \frac{\sum_i R_{si} w_i}{\sum_i w_i}, \tag{23}$$

where the weights are defined by the errors of the individual R_s values $(\Delta R_s)_i$:

$$w_i = \left[\frac{1}{\Delta R_{si}}\right]^2,$$

and the errors of the averaged $\overline{R_s}$ is:

$$\Delta\mathfrak{R} = \frac{1}{\sqrt{\sum_i w_i}}.$$

The effective neutron-proton asymmetry ΔS_{eff} is given by[[12]]

$$\Delta S_{\mathrm{eff}} = S_n + \bar{E}_f - S_p, \text{ for neutron removal,}$$
$$\Delta S_{\mathrm{eff}} = S_p + \bar{E}_f - S_n, \text{ for proton removal,}$$

where $\bar{E}_f$ is obtain by weighting the excitation energy E^* of each final state by the single nucleon removal cross section to that state.

Using the method described in the previous subsection, we analyzed a series of single-nucleon removal reaction data. Details of these reactions, such as the target nuclei used, the incident energies are given in Table. 2. The theoretical predicted single-nucleon removal cross sections using the NTG and the OLA, $\sigma_{-1N}^{\mathrm{NTG}}$ and $\sigma_{-1N}^{\mathrm{OLA}}$, respectively, are also listed together with the experimental single-nucleon removal cross sections, $\sigma_{-1N}^{\mathrm{exp}}$, and the reduction factors, $\mathfrak{R}^{\mathrm{NTG}}$ and $\mathfrak{R}^{\mathrm{OLA}}$, respectively. The single-particle spectroscopic factors (C^2S) used in these calculations are taken from references corresponding to the experimental data and Refs. [43]. These reduction factors are depicted in Fig. 4 as functions of neutron-proton asymmetry. Since many σ_{-1N} were measured inclusively, namely, they include all bound states of the core nuclei, which correspond to different separation energies of the removed nucleon, an effective neutron-proton asymmetry is used here: $\Delta S_{\mathrm{eff}} = S_n + \bar{E}_f - S_p$ for neutron removal and $\Delta S_{\mathrm{eff}} = S_p + \bar{E}_f - S_n$ for proton removal, where $\bar{E}_f$ is the weighted mean excitation energy of the core nucleus, $\bar{E}_f = \left(\sum_i E_{\mathrm{ex,i}}\sigma_{sp,i}\right)/\sum_i \sigma_{sp,i}$, with $E_{\mathrm{ex,i}}$ and $\sigma_{sp,i}$ being the excitation energy of the core nucleus in its i-th state and the corresponding single particle cross section with Eq. (21) [8]. In all these calculations, the single particle wave functions are calculated with Woods-Saxon potentials whose radius parameters, r_0, are determined with the HF calculations [42] and the diffuseness parameters being fixed as

$a = 0.65$ fm except for the ^{15,17,18}C projectiles, for which, the $r_0 = 1.15$ fm and $a = 0.50$ fm is used following Ref. [44]. And for proton removal of ^{16}C, $r_0 = 1.40$ fm and $a = 0.70$ fm is used following Ref. [45]. The proton and neutron density distributions of the nucleus ^{9}Be are taken to be a Gaussian form with a root-mean-square radius of 2.36 fm [9].

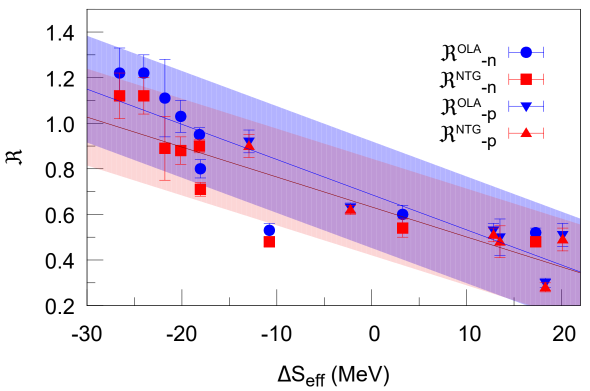

Fig. 4. Averaged reduction factors $\mathfrak{R}$ listed in Table. 2 as functions of the effective neutron-proton asymmetry $\Delta S_{\rm eff}$. The red squares and blue dots are results of the neutron removal of the NTG model and the OLA, respectively. The red triangles and blue inverted triangles are the same but for proton removal. The light red and blue bands represent the widths of their distributions.

As one can see from Table. 2, σ_{-1N} values predicted with the NTG model are generally larger than those with the OLA. Thus, the $\mathfrak{R}$ values with the NTG are smaller than those with the OLA. On average, the changes in the $\mathfrak{R}$ values induced by the NTG model with respect to the OLA are about 7.8%. However, as one can see from Fig. 4, that the $\mathfrak{R}$ values with the NTG model and the OLA, $\mathfrak{R}^{\rm NTG}$ and $\mathfrak{R}^{\rm OLA}$, respectively, still depend linearly on the effective neutron-proton asymmetry $\Delta S_{\rm eff}$, although the slope with the NTG model is 18% smaller than that with the OLA. The parameters of this linear dependence are:

$$\begin{aligned} \mathfrak{R}^{\rm OLA} &= 0.687 - 0.0154\Delta S_{\rm eff}, \\ \mathfrak{R}^{\rm NTG} &= 0.633 - 0.0131\Delta S_{\rm eff}. \end{aligned} \tag{24}$$

So the systematics of the $\mathfrak{R}$ values with respect to $\Delta S_{\rm eff}$ observed in Refs. [8, 9] persist even when the multiple scattering effects inherited in the NTG model are included in the Glauber model calculations.

Looking more closely at Fig. (4), one sees that the differences between $\mathfrak{R}^{\rm NTG}$ and $\mathfrak{R}^{\rm OLA}$ in the most negative $\Delta S_{\rm eff}$ region are larger than at the most positive $\Delta S_{\rm eff}$ region. To be more specific, the averaged differences between $\mathfrak{R}^{\rm NTG}$ and $\mathfrak{R}^{\rm OLA}$ is 9.9% for $\Delta S_{\rm eff} < -10$ MeV and 5.3% for $\Delta S_{\rm eff} > 10$ MeV. This seems to suggest that the multiple scattering effect introduced with the NTG model is more important for removal of weakly bound nucleons than for deeply bound ones. This is misleading. It happens that most of the cases in the $\Delta S_{\rm eff} < -10$ MeV region are single neutron removal reactions, and those in the $\Delta S_{\rm eff} > 10$ MeV region are single proton removal reactions. From the $\mathfrak{R}^{\rm NTG}$ and $\mathfrak{R}^{\rm OLA}$ values shown in Table. 2, one sees that the average differences between $\mathfrak{R}^{\rm NTG}$ and $\mathfrak{R}^{\rm OLA}$ are 10.6% and 4.2% for neutron and proton removal reactions, respectively. Currently, it is not clear why the effect of the NTG model has such systematic differences to these two types of reactions. As we discussed at the end of the last section, the only difference between the NTG model and the OLA is in the core-target S-matrices, S_c. However, as one sees from Eqs. (18) and (19), S_c can not be singled out from S_v and the single-particle wave functions when calculating the single-nucleon removal cross sections. This means that the multiple scattering effects induced in the NTG model to σ_{-1N} through S_c are moderated by the single particle wave functions, which are different for different cases. So we are not able to explicitly show how the NTG model alone affects the σ_{-1N} values and why it behaves differently for proton and neutron removal reactions.

IV. SUMMARY

The reduction of the single-particle strengths, represented by the reduction factors of single-nucleon spectroscopic factors extracted from experimental data with respect to configuration interaction shell model predictions, is supposed to be related to the nucleon-nucleon correlations in atomic nuclei. Quite a lot of theoretical and experimental efforts have been devoted to this area. One of the open questions is why the reduction factors obtained from intermediate- and high-energy single nucleon removal cross sections as those compiled in Refs. [8, 9] show strong linear dependence on the neutron-proton asymmetry, whereas those of other types of reactions, such as (p,pN) and single nucleon transfer reactions do not [2, 3, 6, 59–61]. Since the single-nucleon removal reactions were analyzed with the Glauber model, validity of the Glauber model on such reactions is being questioned. With this respect, corrections to the Glauber model and examination of their effects on the single-nucleon removal cross sections become important.

In this work, we examine how the nucleon-target version of the Glauber model (the NTG model), which introduces multiple scattering of the constituent nucleons in the projectile and the target nuclei, could change the theoretical predicted single-nucleon removal cross sections with respect to the usual optical limit approximation, which does not contain multiple scattering effects. For this purpose, we firstly examined the NTG model in its reproduction of the elastic scattering angular distributions and the total reaction cross sections of the ^{12}C+^{12}C system, and compare their results with the experimental data and those calculated with the OLA. The NTG model is found to improve the description of the elastic scattering angular distributions, especially at lower incident energies. Both the elastic scattering and total reaction cross sections calculated in this work agree well with those reported in previous publications, e.g., Refs. [15, 17, 24].

We then compare the predictions of inclusive single-nucleon removal cross sections by using the NTG model and OLA. The case studied is the ^{9}Be(^{19}C,^{18}C)X reaction within

TABLE 2. Experimental ($\sigma^{\rm exp}_{-1N}$) and theoretical inclusive single-nucleon removal cross sections calculated with the OLA ($\sigma^{\rm OLA}_{-1N}$) and the NTG model ($\sigma^{\rm NTG}_{-1N}$), and the corresponding reductions factors $\mathfrak{R}^{\rm OLA}$ and $\mathfrak{R}^{\rm NTG}$.

Reaction	$\Delta S_{\rm eff}$	Target	$E_{\rm inc}$	$\sigma^{\rm exp}_{-1N}$	$\sigma^{\rm OLA}_{-1N}$	$\sigma^{\rm NTG}_{-1N}$	$\mathfrak{R}^{\rm OLA}$	$\mathfrak{R}^{\rm NTG}$
(^{20}C,^{19}C)	-26.574	C	240	58(5) [46]	47.55	51.88	1.22(11)	1.12(10)
(^{19}C,^{18}C)	-24.142	Be	57	264(80) [47]	179.06	201.62	1.47(45)	1.31(40)
	-24.104	Be	64	226(65) [48]	176.69	195.48	1.28(37)	1.16(33)
	-23.754	C	243	163(12) [46]	134.75	146.63	1.21(9)	1.11(8)
Average	-24.022						1.22(8)	1.12(8)
(^{18}C,^{17}C)	-21.793	C	43	115(18) [44]	103.20	128.70	1.11(17)	0.89(14)
(^{17}C,^{16}C)	-20.130	C	49	84(8) [44]	92.80	109.70	0.91(9)	0.77(7)
	-20.121	Be	62	115(14) [47]	87.80	100.77	1.31(16)	1.14(14)
	-20.121	Be	79	116(18) [49]	90.37	100.48	1.28(20)	1.15(18)
Average	-20.124						1.03(7)	0.88(6)
(^{15}C,^{14}C)	-18.275	C	54	137(16) [44]	180.56	196.44	0.76(9)	0.70(8)
	-18.242	C	62	159(15) [44]	176.11	189.78	0.90(8)	0.84(8)
	-18.169	C	83	146(23) [32]	166.44	176.08	0.88(14)	0.83(13)
	-17.879	Be	103	146(23) [48]	142.52	149.89	0.98(3)	0.94(3)
Average	-18.155						0.95(3)	0.90(0)
(^{16}C,^{15}C)	-18.055	C	55	65(6) [44]	90.90	103.73	0.72(7)	0.63(6)
	-18.053	C	62	77(9) [44]	89.78	101.10	0.86(10)	0.76(9)
	-18.045	Be	75	81(7) [45]	81.99	90.94	0.99(9)	0.89(8)
	-18.094	C	83	65(5) [47]	86.75	94.87	0.75(6)	0.69(5)
Average	-18.051						0.80(4)	0.71(3)
(^{14}C,^{13}C)	-10.807	C	67	65(4) [44]	133.284	148.61	0.49(3)	0.44(3)
	-10.800	C	83	67(14) [32]	130.74	142.66	0.51(13)	0.47(12)
	-10.767	C	235	80(7) [52]	110.92	121.39	0.72(6)	0.66(6)
Average	-10.793						0.53(3)	0.48(2)
(^{12}C,^{11}C)	3.259	C	95	53(22) [55]	102.21	111.06	0.52(22)	0.48(20)
	3.266	C	240	60.51(11.08) [56]	94.12	104.37	0.64(12)	0.58(11)
	3.265	C	250	56.0(41) [54]	93.73	104.31	0.60(4)	0.54(4)
Average	3.263						0.60(4)	0.54(4)
(^{10}C,^{9}C)	17.277	Be	120	23.4(11) [57]	47.40	51.65	0.49(2)	0.45(2)
	17.277	C	120	27.4(13) [57]	49.72	54.36	0.55(3)	0.50(2)
Average	17.277						0.52(2)	0.48(2)
(^{9}C,^{8}B)	-12.925	Be	67	48.6(73) [50]	62.77	66.67	0.77(12)	0.73(11)
	-12.925	Be	100	56(3) [51]	58.77	59.72	0.95(5)	0.94(5)
Average	-12.925						0.92(5)	0.90(5)
(^{12}C,^{11}B)	-2.237	C	230	63.9(66) [53]	103.75	105.33	0.62(6)	0.61(6)
	-2.237	C	250	65.6(26) [54]	102.93	105.36	0.64(3)	0.62(2)
Average	-2.237						0.63(2)	0.62(2)
(^{13}C,^{12}B)	13.523	C	234	39.5(60) [53]	79.69	81.55	0.43(5)	0.40(4)
(^{14}C,^{13}B)	12.830	C	235	41.3(27) [53]	78.65	81.43	0.53(3)	0.51(3)
(^{16}C,^{15}B)	18.303	Be	75	18(2) [45]	60.23	62.50	0.30(3)	0.29(3)
	18.303	Be	239	16(2) [58]	56.86	58.45	0.28(4)	0.27(3)
	18.303	C	239	18(2) [53]	54.57	55.87	0.33(4)	0.32(4)
Average	18.303						0.30(2)	0.28(2)
(^{15}C,^{14}B)	20.134	C	237	28.4(28) [53]	55.36	57.58	0.51(5)	0.49(5)

the incident energy range from 64 to 400 MeV/nucleon. It is found that the σ_{-1n} values predicted with the NTG model are larger than those predicted with the OLA within the whole energy range. The difference is found to be larger at lower incident energies. It will also be larger when the separation energy of the nucleon is larger, which correspond to a smaller root-mean-square radius of the single-particle wave function.

Finally, we study how much the reduction factors of the single particle strengths obtained from single-nucleon removal reactions change when the NTG model is used instead of the OLA. The cases studied are one-nucleon removal reactions induced by $^{9-20}$C isotopes on carbon and ^{9}Be targets. On average, the reduction factors obtained with the NTG model are found to be less than those with the OLA by 7.8%. We also found that the averaged differences in σ_{-1n} are larger than those in σ_{-1p}, which are 10.6% and 4.2%, respectively. However, the linear dependence on the neutron-proton asymmetry of the reduction factors persists. Thus, the question of why the reduction factors of the single particle strengths from single-nucleon removal reaction measurements depend differently on ΔS with respect to other types of reactions remains open even when the multiple scattering effect is included in the Glauber model analysis with the NTG model.

ACKNOWLEDGMENTS

This work was financially supported by the National Key R&D Program of China (Grant No. 2023YFA1606702) and the National Natural Science Foundation of China (Nos. U2067205 and 12205098). We thank Profs. J.A. Tostevin and W. Horiuchi for their helps during this work.

[1] N. K. Glendenning, in *Direct Nuclear Reactions*, (WORLD SCIENTIFIC, 2004)

[2] B. P. Kay, J. P. Schiffer, S. J. Freeman, Quenching of cross sections in nucleon transfer reactions, Phys. Rev. Lett., **111**: 042502 (2013).DOI:10.1103/PhysRevLett.111.042502

[3] B. P. Kay, T. L. Tang, I. A. Tolstukhin,*et al.*, Quenching of single-particle strength in $a = 15$ nuclei, Phys. Rev. Lett., **129**: 152501 (2022).DOI:10.1103/PhysRevLett.129.152501

[4] V. R. Pharipe, I. Sick, P. K. A. d. Huberts, Independent particle motion correlations in fermion systems, Rev. Mod. Phys., **69**,981–991 (1997). DOI:10.1103/RevModPhys.69.981

[5] W. Dickhoff C. Barbieri, Self-consistent green's function method for nuclei nuclear matter, Progress in Particle Nuclear Physics, **52**,377–496 (2004). DOI:10.1016/j.ppnp.2004.02.038

[6] L. Atar, S. Paschalis, C. Barbieri,*et al.*, Quasifree $(p, 2p)$ reactions on oxygen isotopes: Observation of isospin independence of the reduced single-particle strength, Phys. Rev. Lett., **120**: 052501 (2018). DOI:10.1103/PhysRevLett.120.052501

[7] F. Flavigny, N. Keeley, A. Gillibert, A. Obertelli, Single-particle strength from nucleon transfer in oxygen isotopes: Sensitivity to model parameters, Phys. Rev. C, **97**: 034601 (2018). DOI:10.1103/PhysRevC.97.034601

[8] J. A. Tostevin A. Gade, Systematics of intermediate-energy single-nucleon removal cross sections, Phys. Rev. C, **90**: 057602 (2014). DOI:10.1103/PhysRevC.90.057602

[9] J. A. Tostevin A. Gade, Updated systematics of intermediate-energy single-nucleon removal cross sections, Phys. Rev. C, **103**: 054610 (2021).DOI:10.1103/PhysRevC.103.054610

[10] P. Hansen J. Tostevin, Direct reactions with exotic nuclei, Annual Review of Nuclear Particle Science, **53** :219–261 (2003). DOI:10.1146/annurev.nucl.53.041002.110406

[11] T. Pohl, Y. L. Sun, A. Obertelli, *et al.*, Multiple mechanisms in proton-induced nucleon removal at ~ 100 MeV/Nucleon, Phys. Rev. Lett., **130**: 172501 (2023). DOI:10.1103/PhysRevLett.130.172501

[12] E. C. Simpson J. A. Tostevin, One- two-neutron removal from the neutron-rich carbon isotopes, Phys. Rev. C, **79**: 024616 (2009). DOI:10.1103/PhysRevC.79.024616

[13] C. Bertulani, Core destruction in knockout reactions, Physics Letters B, **846**: 138250 (2023). DOI:10.1016/j.physletb.2023.138250

[14] Y. Suzuki, K. Yabana, R. G. Lovas, K. Varga, in *Structure Reactions of Light Exotic Nuclei*, (Taylor & Francis, 2003).

[15] B. Abu-Ibrahim Y. Suzuki, Scatterings of complex nuclei in the glauber model, Phys. Rev. C, **62**: 034608 (2000). DOI:10.1103/PhysRevC.62.034608

[16] B. Abu-Ibrahim Y. Suzuki, Utility of nucleon-target profile function in cross section calculations, Phys. Rev. C, **61**: 051601 (2000).DOI:10.1103/PhysRevC.61.051601

[17] W. Horiuchi1, Y. Suzuki, B. Abu-Ibrahim *et,al.*, Systematic analysis of reaction cross sections of carbon isotopes, Phys. Rev. C, **76**: 044607 (2007).DOI:10.1103/PhysRevC.75.044607

[18] R. J. Glauber, in *Lectures on Theoretical Physics*, (Interscience, New York, 1959)

[19] S. Hatakeyama, S. Ebata, W. Horiuchi, and M. Kimura, Multiple-scattering effects in proton- and alpha-nucleus reactions with Glauber theory, J. Phys. Conf. Ser., **569**: 012050 (2014).doi:10.1088/1742-6596/569/1/012050

[20] L. Ray, Proton-nucleus total cross sections in the intermediate energy range, Phys. Rev. C, **20**:1857–1872, (1979). DOI:10.1103/PhysRevC.20.1857

[21] C. Werneth, X. Xu, R. Norman, W. Ford, K. Maung, Validation of elastic cross section models for space radiation applications, Nuclear Instruments Methods in Physics Research Section B: Beam Interactions with Materials Atoms, **392**,74–93 (2017). DOI:10.1016/j.nimb.2016.12.009

[22] R. L. Workman *et,al.*, Review of particle physics, PTEP, **2022**: 083C01 (2022). DOI:10.1093/ptep/ptac097

[23] J. A. Tostevin, Cross sections of removal reactions populating weakly-bound residual nuclei , (2022). DOI:10.48550/arXiv.2203.06058

[24] T. Nagahisa W. Horiuchi, Examination of the ^{22}C radius determination with interaction cross sections, Phys. Rev. C, **97**: 054614 (2018). DOI:10.1103/PhysRevC.97.054614

[25] C. Bertulani A. Gade, Momdis: a glauber model computer code for knockout reactions, Computer Physics Communications, **175** ,372–380 (2006). DOI:10.1016/j.cpc.2006.04.006

[26] J.A. Tostevin, M.H. Lopes, and R.C. Johnson, Elastic scattering and deuteron-induced transfer reactions, Nucl. Phys. A, **465**: 83-122 (1984). DOI:10.1016/0375-9474(87)90300-9

[27] M. Takechi, M. Fukuda, M. Mihara, *et. al.,* Reaction cross sections at intermediate energies and Fermi-motion effect, Phys. Rev. C, **79**: 061601(R) (2009).

DOI:10.1103/PhysRevC.79.061601

[28] Y.H. Wang, D.Y. Pang, W.D. Chen, *et. al.,* Nuclear radii from total reaction cross section measurements at intermediate energies with complex turning point corrections to the eikonal model, Phys. Rev. C, **109**: 014621 (2024). DOI:10.1103/PhysRevC.109.014621

[29] J. Hostachy, M. Buenerd, J. Chauvin,*et,al.*, Elastic inelastic scattering of 12c ions at intermediate energies, Nucl. Phys. A, **490**,441–470 (1988). DOI:10.1016/0375-9474(88)90514-3

[30] M. Buenerd, A. Lounis, J. Chauvin, D. Lebrun: Martin, G. Duhamel, J. Gondr, P. De Saintignon, Elastic inelastic scattering of carbon ions at intermediate energies, Nucl. Phys. A, **424**: 313–334 (1984). DOI:10.1016/0375-9474(84)90186-6

[31] D.T. Khoa, α-nucleus optical potential in the double-folding model, Phys. Rev. C, **63**: 034007 (2018). DOI:10.1103/PhysRevC.63.034007

[32] D. Q. Fang, T. Yamaguchi, T. Zheng, *et al.*, One-neutron halo structure in ^{15}C, Phys. Rev. C, **69**: 034613 (2004). DOI:10.1103/PhysRevC.69.034613

[33] S. Kox, A. Gamp, C. Perrin, *et al.*, Trends of total reaction cross sections for heavy ion collisions in the intermediate energy range, Phys. Rev. C, **35**,1678–1691 (1987). DOI:10.1103/PhysRevC.35.1678

[34] J. Jaros, A. Wagner, L. erson,*et al*, Nucleus-nucleus total cross sections for light nuclei at 1.55 2.89 gev/c per nucleon, Phys. Rev. C, **18**,2273–2292 (1978). DOI:10.1103/PhysRevC.18.2273

[35] T. Zheng, T. Yamaguchi, A. Ozawa, *et al.*, Study of halo structure of 16c from reaction cross section measurement, Nuclear Physics A, **709**, 103–118 (2002). DOI:10.1016/S0375-9474(02)01043-6

[36] H. Zhang, W. Shen, Z. Ren, *et al.*, Measurement of reaction cross section for proton-rich nuclei (a<30) at intermediate energies, Nuclear Physics A, **707**, 303–324 (2002). DOI:10.1016/S0375-9474(02)01007-2

[37] C. Perrin, S. Kox, N. Longequeue, *et al.*, Direct measurement of the ^{12}C + ^{12}C reaction cross section between 10 83 mev/nucleon, Phys. Rev. Lett., **49**, 1905–1909, (1982). DOI:10.1103/PhysRevLett.49.1905

[38] M. Takechi, M. Fukuda, M. Mihara, *et al.*, Reaction cross-sections for stable nuclei nucleon density distribution of proton drip-line nucleus 8B, The European Physical Journal A, **25**, 217–219, (2005). DOI:10.1140/epjad/i2005-06-078-0

[39] L. Ponnath, T. Aumann, C. Bertulani, *et al.*, Measurement of nuclear interaction cross sections towards neutron-skin thickness determination, Physics Letters B, **855**:138780 (2024). DOI:10.1016/j.physletb.2024.138780

[40] K. Hencken, G. Bertsch, H. Esbensen, Breakup reactions of the halo nuclei ^{11}Be ^{8}B, Phys. Rev. C, **54**, 3043–3050 (1996). DOI:10.1103/PhysRevC.54.3043

[41] A.E.L. Dieperink and T. de Forest, Phys. Rev. C 10, 543 (1974).DOI: https://doi.org/10.1103/PhysRevC.10.543

[42] W. L. Hai, D. Y. Pang, X. B. Wang, *et al.*, Determining the radii of single particle potentials with skyrme hartree fock calculations, Phys. Rev. C,**110**:044613 (2024). DOI:10.1103/PhysRevC.110.044613

[43] Y.-P. Xu, D.-Y. Pang, C.-X. Yuan, X.-Y. Yun, Quenching of single-particle strengths of carbon isotopes 9-12,14-20c with knockout reactions for incident energies 43-2100 mev/nucleon *, Chinese Physics C, **46**: 064102 (2022). DOI:10.1088/1674-1137/ac5236

[44] E. Sauvan, F. Carstoiu, N. A. Orr,*et al.*, One-neutron removal reactions on light neutron-rich nuclei, Phys. Rev. C, **69**: 044603 (2004).DOI:10.1103/PhysRevC.69.044603

[45] F. Flavigny, A. Obertelli, A. Bonaccorso, *et al.*, Nonsudden limits of heavy-ion induced knockout reactions, Phys. Rev. Lett., **108**: 252501 (2012). DOI:10.1103/PhysRevLett.108.252501

[46] N. Kobayashi, T. Nakamura, J. A. Tostevin,*et al.*, One-two-neutron removal reactions from the most neutron-rich carbon isotopes, Phys. Rev. C, **86**: 054604 (2012). DOI:10.1103/PhysRevC.86.054604

[47] V. Maddalena, T. Aumann, D. Bazin, *et al.*, Single-neutron knockout reactions: Application to the spectroscopy of ^{16,17,19}C, Phys. Rev. C, **63**: 024613 (2001). DOI:10.1103/PhysRevC.63.024613

[48] J. R. Terry, D. Bazin, B. A. Brown,*et al.*, Absolute spectroscopic factors from neutron knockout on the halo nucleus ^{15}C, Phys. Rev. C, **69**: 054306 (2004). DOI:10.1103/PhysRevC.69.054306

[49] C. Wu, Y. Yamaguchi, A. Ozawa, I. Tanihata, D. Jiang, H. Hua, T. Zheng, Z. Li, Y. Ye, Neutron removal reactions of 17c, Journal of Physics G: Nuclear Particle Physics, **31**: 39 (2004). DOI:10.1088/0954-3899/31/1/004

[50] R. J. Charity, L. G. Sobotka, J. A. Tostevin, Single-nucleon knockout cross sections for reactions producing resonance states at or beyond the drip line, Phys. Rev. C, **102**: 044614 (2020). DOI:10.1103/PhysRevC.102.044614

[51] D. Bazin, R. J. Charity, R. T. de Souza,*et al.*, Mechanisms in knockout reactions, Phys. Rev. Lett., **102**: 232501 (2009). DOI:10.1103/PhysRevLett.102.232501

[52] Y. Z. Sun, S. T. Wang, Z. Y. Sun, *et al.*, Single-neutron removal from ^{14,15,16}C near 240 mev/nucleon, Phys. Rev. C, **104**: 014310 (2021). DOI:10.1103/physrevc.104.014310

[53] Y. Z. Sun, S. T. Wang, Z. Y. Sun, *et al.*, One-proton removal from neutron-rich carbon isotopes in $^{12--16}$C beams near 240 mev/nucleon beam energy, Phys. Rev. C, **11**0: 014603 (2024). DOI:10.1103/PhysRevC.110.014603

[54] B. A. Brown: G. Hansen, B. M. Sherrill, J. A. Tostevin, Absolute spectroscopic factors from nuclear knockout reactions, Phys. Rev. C, **65**: 061601 (2002). DOI:10.1103/PhysRevC.65.061601

[55] J. Dudouet, D. Juliani, M. Labalme, *et al.*, Double-differential fragmentation cross-section measurements of 95 mev/nucleon ^{12}c beams on thin targets for hadron therapy, Phys. Rev. C, **88**: 024606 (2013). DOI:10.1103/PhysRevC.88.024606

[56] Y. SUN, Y. ZHAO, S. JIN, *et al.*, Data analysis framework for radioactive ion beam experiments at the external target facility of hirfl-csr, Nuclear Physics Review, **37**: 742 (2020). DOI:10.11804/NuclPhysRev.37.2019CNPC27

[57] G. F. Grinyer, D. Bazin, A. Gade, *et al.*, Systematic study of p-shell nuclei via single-nucleon knockout reactions, Phys. Rev. C, **86**: 024315 2012. DOI:10.1103/PhysRevC.86.024315

[58] Y. X. Zhao, Y. Z. Sun, S. T. Wang,*et al.*, One-proton knockout from ^{16}C at around 240 mev/nucleon, Phys. Rev. C, **100**: 044609 (2019). DOI:10.1103/PhysRevC.100.044609

[59] F. Flavigny, A. Gillibert, L. Nalpas, *et al.*, Limited asymmetry dependence of correlations from single nucleon transfer, Phys. Rev. Lett., **110**: 122503 (2013). DOI:10.1103/PhysRevLett.110.122503

[60] M. Gómez-Ramos A. Moro, Binding-energy independence of reduced spectroscopic strengths derived from (p,2p) (p,pn) reactions with nitrogen oxygen isotopes, Physics Letters B, **785**, 511–516 (2018). DOI:10.1016/j.physletb.2018.08.058

[61] Y.P. Xu, D.Y. Pang, X.Y. Yun, *et al.*, Proton–neutron asymmetry independence of reduced single-particle strengths derived

from (p,d) reactions, Physics Letters B, **790**, 308–313 (2019). DOI:10.1016/j.physletb.2019.01.034